frontiers in Materials

ORIGINAL RESEARCH
published: 11 June 2021
doi: 10.3389/fmats.2021.687562

Temperature Controlled Evolution of Pure Phase Cu_9S_5 Nanoparticles by Solvothermal Process

Olalekan C. Olatunde[1,2] *and Damian C. Onwudiwe*[1,2]*

[1]*Material Science Innovation and Modelling (MaSIM) Research Focus Area, Faculty of Natural and Agricultural Science, North-West University (Mafikeng Campus), Mmabatho, South Africa,* [2]*Department of Chemistry, Faculty of Natural and Agricultural, Science, North-West University (Mafikeng Campus), Mmabatho, South Africa*

Copper sulphides are one of the most explored semiconductor metal sulphides because of their stoichiometric and morphological dependent optical and electrical properties, which makes them tunable for numerous optoelectronic applications. Stoichiometrically, copper sulphides exist in numerous structures which varies from the copper-rich phase (Cu_2S) to the copper-deficient phase (CuS). Within these extreme stoichiometric phases lies numerous non-stoichiometric phases with interesting optical properties. Different solvothermal techniques have been explored for the synthesis of copper sulphides; however, the thermal decomposition of single source precursors provides a facile and tunable route to the synthesis of pure phase copper sulphides of different stoichiometries. In this study, copper (II) dithiocarbamate have been explored as a single source precursor compound to study the evolution of pure phase Cu_9S_5. Below 240°C, mixed phase of CuS and Cu_9S_5 were obtained, and as the temperature was increased beyond 240°C, keeping other reaction condition unchanged, the precursor yielded pure phase of Cu_9S_5. This phase selectivity at high temperature was attributed to the increased reducing ability of oleylamine (used as solvent) which enhance the evolution of the copper rich phase at high temperature. Optical and morphological studies of the pure phase Cu_9S_5, showed properties that varied considerably with the temperature of synthesis.

Keywords: copper sulphide, precursor route, phase evolution, optical, morphology, stoichiometric composition

Edited by:
Zhiyong Gao,
Central South University, China

Reviewed by:
Rajkumar Kaliyamoorthy,
SSN College of Engineering, India
Hongjin Lv,
Beijing Institute of Technology, China

***Correspondence:**
Damian C. Onwudiwe
Damian.Onwudiwe@nwu.ac.za

Specialty section:
This article was submitted to Colloidal Materials and Interfaces, a section of the journal Frontiers in Materials

Received: *29 March 2021*
Accepted: *27 May 2021*
Published: *11 June 2021*

Citation:
Olatunde OC and Onwudiwe DC (2021) Temperature Controlled Evolution of Pure Phase Cu_9S_5 Nanoparticles by Solvothermal Process. Front. Mater. 8:687562. doi: 10.3389/fmats.2021.687562

INTRODUCTION

The unique properties of semiconductor nanoparticles have made them a subject of intense research in recent time. These properties are strongly influenced by their morphology, phase and surface characteristics. Their potential application in various fields such as catalysis (Shanmugam et al., 2020), non-linear optics (Chen et al., 2014), photoelectrochemistry (Hao et al., 2020), light emitting diodes (Chen et al., 2020) and biosensing (Yue et al., 2020) is dependent on the ability to manipulate these properties by controlling their size, shape and phase.

Metal nitrides, oxynitrides, oxides and sulphides are among the well explored semiconductors, with oxides and sulphides being the most studied materials among them. However, most metal oxides are wide band gap semiconductors, due to their valence band comprising of a deep 2p oxygen orbital and the high effective mass of the hole carriers resulting from oxygen's 2p localization state (Raebiger et al., 2007; Shiga et al., 2016; Chandrasekaran et al., 2019). Metal sulphides have therefore inspired great interest as semiconductors because of their suitable band position and electronic band

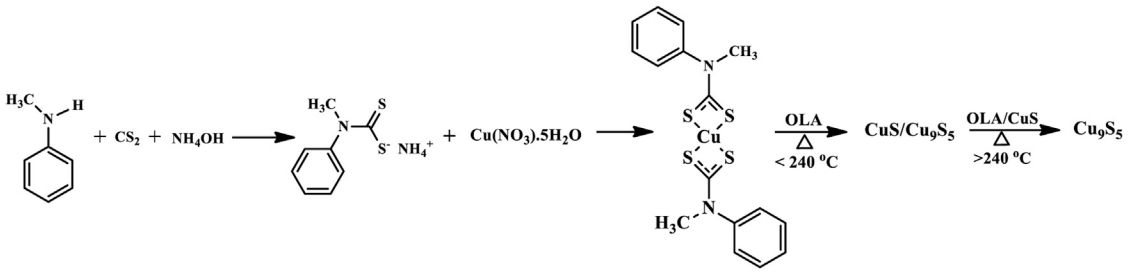

SCHEME 1 | Synthesis of pure phase Cu_9S_5 from copper (II) bis(*N*-methyl-*N*-phenyl dithiocarbamate) single source precursor.

gap. The ability of the sulphides to also exist in a variety of morphologies, and stoichiometries with excellent optical characteristics makes them potential materials in a variety of devices such as thermoelectric devices (Chen et al., 2019), fuel cells, solar cells (Suárez et al., 2017), sensors (Zhao et al., 2020), lithium-ion batteries, non-volatile memory devices (Mazor et al., 2009) and light-emitting diodes (Yoo and Kim, 2009).

Copper sulphides ($Cu_{2-x}S$) are one of the most studied semiconductor metal sulphides due to its wide range of stoichiometric compositions and phases, which influence their optical and electrical properties (Zhang et al., 2019). They are excellent p-type semiconductors, a consequence of the copper vacancies in the crystal lattice, and exhibit a stoichiometry dependent bandgap range of 1.2–2.0 eV (Han et al., 2016). Some of the identified stoichiometries with their band gap energies include chalcocite (Cu_2S), 1.2 eV; digentite ($Cu_{1.8}S$ or Cu_9S_5), 1.55 eV; djurleite ($Cu_{1.95}S$), 1.3 eV; anilite ($Cu_{1.75}S$ or Cu_7S_4), 1.70 eV; and covellite (CuS), 2.0 eV (Abdelhady et al., 2011; Li et al., 2017). Cu_9S_5 crystallizes in the hexagonal digentite phase and has been explored in a variety of technologies such as solar cells and in sodium-ion batteries (Jing et al., 2018). It has also showed potential as materials in thermoelectronics (Zhu and Wang, 2019), photoelectrochemicals and sensors (Cheng et al., 2019).

Development of synthetic routes to copper sulphides is still a rigorously researched area because methods that could offer control over the stoichiometry of the produced materials are still well sought. Some of the methods that have been explored for the synthesis of $Cu_{2-x}S$ are based on techniques which includes ultrasound (Behboudnia and Khanbabaee, 2007), subcritical and supercritical (Li et al., 2018), mechanochemical (Li et al., 2016), microwave (Zhang et al., 2002), pyrolysis (Jing et al., 2018) and solvothermal (Motaung et al., 2019). Solvothermal synthesis is a widely used route due to the great influence on morphology that it affords by virtue of its moderate temperature requirement. The process also involves the use of environmentally benign solvents (Motaung et al., 2019). The choice of precursors plays an important role on the final stoichiometry and phase of the nanomaterial synthesized. The use of single source precursors in the synthesis of nanoparticles have gained increased attention as it offers monodispersed products via a safe, mild and simple process (Malik et al., 2001). Some of the complexes that have been explored as precursor compounds include dithiocarbamates (Zhu and Wang, 2019), thiadiazole (Cheng et al., 2019), carbamothioyl (Saeed et al., 2013) and thioubuiret (Abdelhady et al., 2011). In this present work, copper (II) bis(*N*-methyl-*N*-phenyl dithiocarbamate) was utilised as single source precursor to prepare pure phase digentite by controlling the temperature of the reaction in the presence of oleylamine (OLA). The aim was to study the role of temperature in the evolution of pure phase of copper sulphide nanoparticles using a dithiocarbamate complex.

EXPERIMENT SECTION

Materials

Cu(II) nitrate pentahydrate, carbon disulphide, oleylamine, methanol, toluene, N-methyl aniline, and ammonium solution used were all of analytical grade and used as supplied by Merck.

Synthesis of Ammonium *N*-methyl-*N*-phenyl Dithiocarbamate Ligand

A previously reported method was used for the synthesis of the ammonium *N*–methyl–*N*–phenyl dithiocarbamate (Onwudiwe and Ajibade, 2010). Briefly, 0.05 mol of carbon disulphide was added into an ice-cold mixture of 0.05 mol *N*-methyl aniline and 15 ml of concentrated aqueous ammonia. The resulting solution was stirred vigorously for 6–7 h, to obtain a yellowish solid product which was filtered by suction and rinsed three times with 75 ml of cold ethanol.

Synthesis of Cu (II) bis *N*-methyl-*N*-phenyl Dithiocarbamate

Aqueous solutions of the ligand and metal salt in mole ratio of 2:1 were stirred together at ambient temperature for 1 h. The dark brown precipitate formed was filtered and washed severally with water and ethanol. The precipitate was allowed to dry overnight under vacuum and stored for further use.

Synthesis of Cu_9S_5 Nanoparticles

The nanoparticles were prepared using the Alton Paar monowave 50 reactor. In a typical synthesis, a specific amount of the precursor complex and 10 ml of oleylamine were introduced into the reactor tube and stirred to form a slurry. The reactor tube was then placed in the tube chamber and heated to the desired temperature of 200, 220, 240, 260, and 280°C. The reactor was allowed to run for 1 h and then left to cool down. The

obtained nanoparticles were rinsed in a mixture of toluene and ethanol by centrifuging to remove excess capping agent and then dispersed in ethanol to obtain the sample solution for characterization. **Scheme 1** shows the synthesis steps for obtaining the pure phase Cu_9S_5.

Characterization

XRD spectra of the samples was measured with Phillips X'pert diffractometer with a secondary graphite monochromated Cu Kα radiation (λ = 1.546 Å) at 40 kV/50 mA. PerkinElmer λ20 UV-vis spectrophotometer was used for the UV/visible measurements. The photoluminescence properties were studied using Perkin Elmer LS 45 fluorimeter. Scanning electron microscopy (SEM) and transmission electron microscopy (TEM) were used to study the morphology of the samples using FEI Quanta FEG 250 Environmental Scanning electronmicroscope (ESEM) and a TECNAI G2 (ACI) equipment (Hillsboro, OR, United States) respectively.

RESULTS AND DISCUSSION

X-Ray Diffraction Studies of the Nanoparticles

The XRD patterns of the products obtained after the thermolysis of the copper complex in OLA at different temperatures from 200–280°C are shown in **Figure 1**. The patterns showed that a gradual evolution of digenite pure phase occurred as the thermolysis temperature was increased. At 200°C, peaks that could be indexed to both CuS and Cu_9S_5 phases were observed. A reduction in the CuS peaks occurred with concomitant increase in the peak intensity of the Cu_9S_5 phase as the temperature was increased to 220°C. A further increase in temperature to 240°C, showed that a pure phase was obtained with peaks indexed to the rhombohedral Cu_9S_5 (JCPDS card No. 47–1748, space group: R$\bar{3}$m (166), lattice constant: a = b = 3.930 Å, c = 48.140 Å and $\alpha = \beta = 90^o$, $\gamma = 120^o$) (Wang et al., 2015). Beyond the 240°C, the pure phase remained constant, with a slight shift of the 111 peak to high wavelength region which could be attributed to change in crystallite size and lattice strain (Khorsand Zak et al., 2011).

OLA has been reported to possess the ability to play the role not only as capping molecules and solvent in nanoparticle synthesis, but the presence of nitrogen confers on it some electron donating and reducing capabilities. The high affinity of the amine group accounts for OLA's fast interaction and its general tendency to produce large particle size and wide shape variety (Mbewana-Ntshanka et al., 2020). The reducibility of OLA has recently been reported as an important factor in controlling the Cu^{2+}/Cu^{+} kinetics and reactions between $Cu_{2-x}S$ clusters and Cu^{+}, which are important in phase selectivity of $Cu_{2-x}S$ (Fu et al., 2015). In the stoichiometric phase, Cu_2S, Cu^{+} are located at trigonal centres of S^{2-}. The Cu^{+} in this phase is highly mobile even at ambient temperature, generating holes in the valence band and increase in under coordinated S^{-1} (Liu et al., 2019). With increased accumulation of S^{-1}, disulphide bonds are formed and the Cu^{+} are more favoured to occupy tetrahedral centres leading to mobility loss. Among copper sulphide phases, covellite (CuS) possess the highest hole concentration and the lowest Cu:S ratio, accounting for the slow mobility of Cu ion due to their tetrahedral coordination and increased disulphide bond. This disulphide bond could be reduced in the presence of reducing species or cations in lower oxidation states. Studies by Liu et al. (2017), Fu et al. (2015), have shown that at low temperatures and with sufficient amount of S, the CuS phase is the most favoured, which accounts for the mixed phases obtained at temperatures below 220°C in the present study. As the temperature of the system was increased, the reducing ability of OLA was enhanced (Tyagi et al., 2019) and a reduction of the disulphide bond in CuS leads to the conversion of the CuS phase to the Cu_9S_5 phase, which was achieved at 240°C.

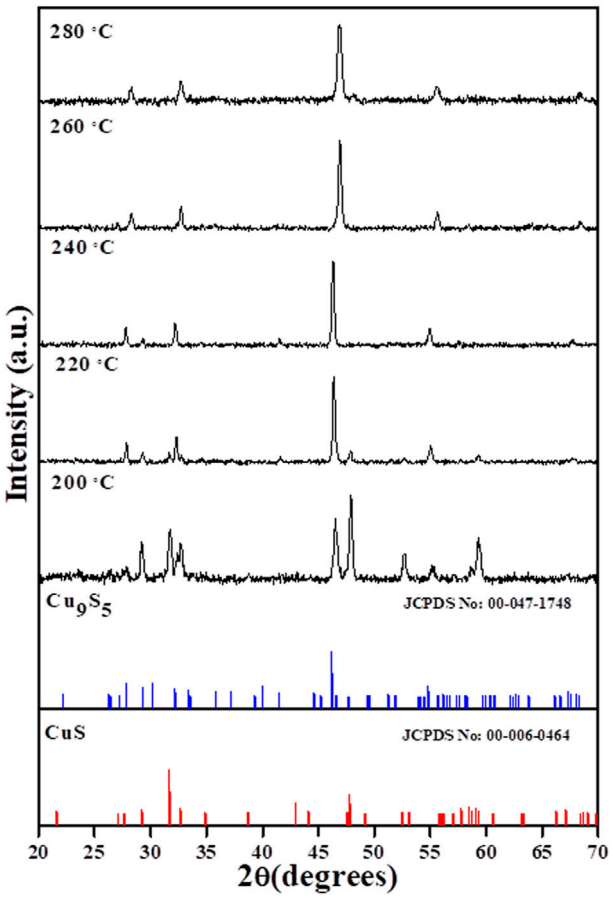

FIGURE 1 | XRD pattern of the copper sulfide nanoparticles obtained by the thermolysis of Cu(II) bis(*N*-methyl-*N*-phenyl dithiocarbamate) in the temperature range of 200–280°C.

Morphological Studies

The TEM images of the pure phase Cu_9S_5 obtained at 240, 260, and 280°C are shown in **Figure 2**. The nanoparticles were rectangular-shaped at all the temperatures and showed a decrease in size as temperature increases. The length of the nanoparticles was 176 ± 51.9, 111.6 ± 21.1, and 82.1 ± 21.8 nm. Thus, a narrower size distribution was obtained at higher temperature. Measurement of the width of the cubes

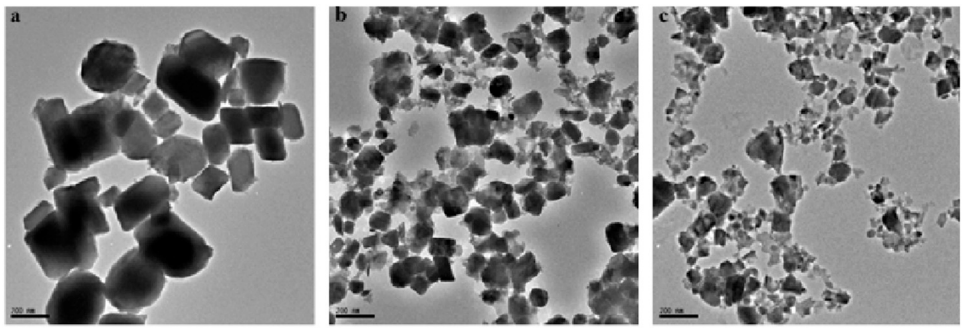

FIGURE 2 | TEM images of pure phase Cu_9S_5 obtained at **(A)** 240°C **(B)** 260°C and **(C)** 280°C using Cu(II) bis(*N*-methyl-*N*-phenyl dithiocarbamate) as single source precursor.

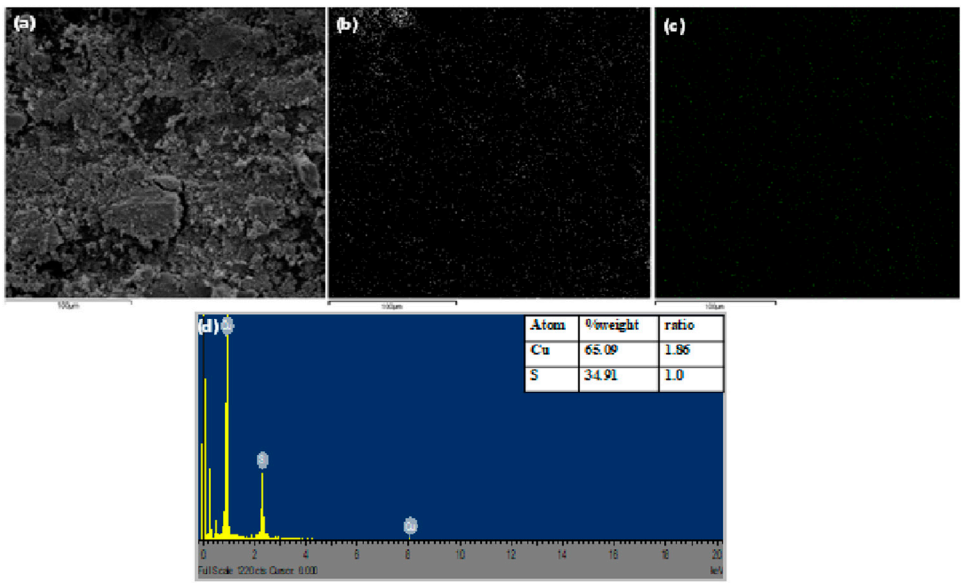

FIGURE 3 | (A) SEM image of Cu_9S_5 **(B,C)** elemental mapping of Cu and S respectively, and **(D)** EDX spectra of Cu_9S_5.

also showed a gradual decrease in width with increase in temperature. The obtained values were 34.7 ± 13.3, 12.9 ± 2.3, and 12.1 ± 5.2 nm at 240, 260, and 280°C respectively. Generally increases, it has been established that in wet chemical synthesis, nucleation of nanoparticles is enhanced at high temperatures, while particle growth is more favored at relatively lower temperature. Thus, particles with larger size were obtained at low temperatures, with a decrease in particle size as temperature increase (Liu et al., 2020).

The SEM, elemental mapping image and EDS spectra of the pure Cu_9S_5 obtained at 280°C are shown in **Figure 3**. The surface morphology of the nanoparticles presented in the SEM micrograph showed spherical particles that were agglomerated due to the high surface reactivity. **Figures 3B,C** are the elemental mapping images showing the uniform distribution of Cu and S in the nanoparticle. From the EDS spectra, it could be confirmed that the primary elemental constituent of the nanoparticles was copper and sulphur in molar ratio of 1.87:1 (Cu/S), which was in close agreement with the stoichiometric ratio in the digenite phase.

Optical Properties

The optical properties of the synthesized nanoparticles were studied by measuring the absorbance using the UV-vis spectrophotometer and the corresponding Tauc plots were obtained as shown in **Figure 4**, using the equation (Tauc et al., 1966):

$$\alpha h\nu \propto \left(h\nu - E_g\right)^n \quad (1)$$

Where ν is the light frequency, h is the plank constant, α is the absorption coefficient of the material and E_g represents the band gap. The exponent n indicates the nature of the band-gap and it can take values of 2, ½, 2/3, and 1/3, which corresponds to direct allowed, indirect allowed, forbidden direct and forbidden indirect transitions respectively. The band gap E_g of the nanoparticles were obtained by

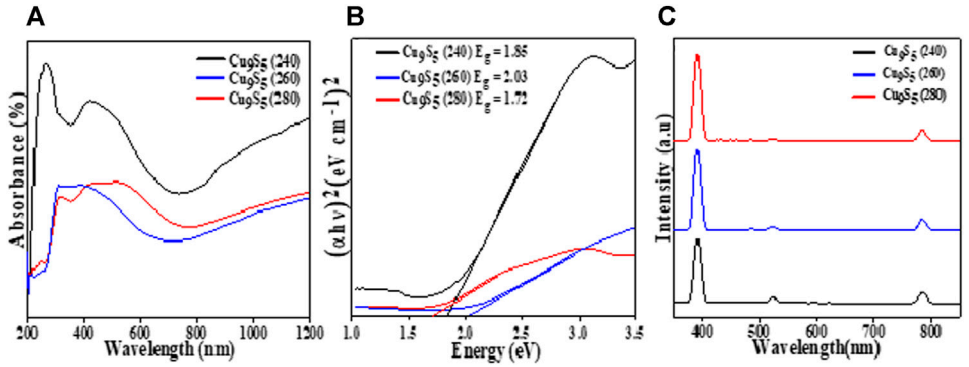

FIGURE 4 | Optical properties of Cu_9S_5 obtained from Cu(II) bis(*N*-methyl-*N*-phenyl dithiocarbamate) as single source precursor: **(A)** Absorption spectra, **(B)** Tauc plots and **(C)** Photoluminescence spectra.

extrapolating the linear portion of the plots $(\alpha h\nu)^2$ against hν to $\alpha = 0$. Currently, there is no general consensus on the nature of transitions for most $Cu_{2-x}S$ phases, leading to both direct and indirect transitions being reported for most phases (Pop et al., 2011). A large range of band gap energy have been reported for different $Cu_{2-x}S$ phases, which arises due to the large number of mixed phases and compositions coupled with different crystal size and shapes (Safrani et al., 2013).

All the samples exhibited broad absorption in the visible region (300–500 nm) and tailed into the near infra-red region (**Figure 4A**). The absorption onset for the three samples was at ~ 350 nm and the spectra showed an increase in absorbance in the near edge region indicating that the bandgap value will be obtained in the near infra-red region (Adekoya et al., 2019). The increase in absorption at higher wavelengths may be ascribed to free-carrier intra-band absorbance (Zhao et al., 2009). The direct band gap for the three samples were 1.85, 2.03, and 1.72 eV for the Cu_9S_5 samples obtained at 240, 260, and 280°C respectively, which are in agreement with values previously reported in literature (Senthilkumar and Babu, 2016; Li et al., 2017; Itzhak et al., 2018). This difference in band gaps for the samples could be attributed to difference in size, stoichiometric variation and the arrangement of the cations and anions in the atomic structure of the compounds.

The emission spectra of the ethanol solution of the Cu_9S_5 samples irradiated at 800 nm is shown in **Figure 4C**. The three nanostructures showed similar emission spectra with three peaks observed at 390, 522, and 783 nm which corresponded to energy values of 3.2, 2.3, and 1.57 eV respectively. These observed peaks are in agreement with the absorption spectra of the samples and the peak at 390 nm could be assigned to the near band edge emission. The peaks at 522 and 783 nm both corresponds to the band to band transitions in the Cu_9S_5 nanoparticles.

CONCLUSION

The synthesis of pure phase Cu_9S_5 using a single source precursor route was explored and the optical and morphological properties of the obtained nanoparticles were studied. The synthetic route was observed to induce a selectivity in the stoichiometric phase by changing the reaction temperature, which also influenced the properties of the OLA employed as solvent and capping agent in the reaction system. The obtained materials showed varying morphological, and optical properties with change in temperature. The band gap energy for the nanoparticles varied between 1.72–2.03 eV in the temperature range studied. While the nanoparticles exhibited similar morphology, their dimension varied with temperature. The length and width of the nanoparticles decreased with increasing temperature with dimensions in the range of 82–179 nm and 12–34 nm for the length and width respectively. This study showed the possibility of selectively tuning the phase purity of $Cu_{2-x}S$ prepared through the single source precursor route by altering the reaction temperature, which results in the solvent property modification and enhanced phase selectivity.

DATA AVAILABILITY STATEMENT

The original contributions presented in the study are included in the article/Supplementary Material, further inquiries can be directed to the corresponding author.

AUTHOR CONTRIBUTIONS

OO carried out laboratory experiments and wrote the first draft of the manuscript. DO supervised the project, read and revised the manuscript drafts.

FUNDING

Financial assistance (1K02799) from the North-West University is gratefully acknowledged.

REFERENCES

Abdelhady, A. L., Ramasamy, K., Malik, M. A., O'Brien, P., Haigh, S. J., and Raftery, J. (2011). New Routes to Copper Sulfide Nanostructures and Thin Films. *J. Mater. Chem.* 21 (44), 17888–17895. doi:10.1039/c1jm13277f

Adekoya, J. A., Khan, M. D., and Revaprasadu, N. (2019). Phase Transition in Cu2+xSnS3+y ($0 \le X \le 2$; $0 \le Y \le 1$) Ternary Systems Synthesized from Complexes of Coumarin Derived Thiocarbamate Motifs: Optical and Morphological Properties. *RSC Adv.* 9 (61), 35706–35716. doi:10.1039/c9ra07376k

Behboudnia, M., and Khanbabaee, B. (2007). Investigation of Nanocrystalline Copper Sulfide Cu7S4 Fabricated by Ultrasonic Radiation Technique. *J. Cryst. Growth* 304 (1), 158–162. doi:10.1016/j.jcrysgro.2007.02.016

Chandrasekaran, S., Zhang, P., Peng, F., Bowen, C., Huo, J., and Deng, L. (2019). Tailoring the Geometric and Electronic Structure of Tungsten Oxide with Manganese or Vanadium Doping toward Highly Efficient Electrochemical and Photoelectrochemical Water Splitting. *J. Mater. Chem. A.* 7 (11), 6161–6172. doi:10.1039/c8ta12238e

Chen, J. L. T., Nalla, V., Kannaiyan, G., Mamidala, V., Ji, W., and Vittal, J. J. (2014). Synthesis and Nonlinear Optical Switching of Bi2S3 Nanorods and Enhancement in the NLO Response of Bi2S3@Au Nanorod-Composites. *New J. Chem.* 38 (3), 985–992. doi:10.1039/c3nj01380d

Chen, W.-C., Shiao, J.-H., Tsai, T.-L., Jiang, D.-H., Chen, L.-C., Chang, C.-H., et al. (2020). Multiple Scattering from Electrospun Nanofibers with Embedded Silver Nanoparticles of Tunable Shape for Random Lasers and White-Light-Emitting Diodes. *ACS Appl. Mater. Inter.* 12 (2), 2783–2792. doi:10.1021/acsami.9b16059

Chen, X., Zhang, H., Zhao, Y., Liu, W.-D., Dai, W., Wu, T., et al. (2019). Carbon-Encapsulated Copper Sulfide Leading to Enhanced Thermoelectric Properties. *ACS Appl. Mater. Inter.* 11 (25), 22457–22463. doi:10.1021/acsami.9b06212

Cheng, Y., Deng, S., Sun, F., and Zhou, Y.-H. (2019). Synthesis of Luminescent Cu9S5 Nanoclusters from Copper-2,5-Dimercapto-1,3,4-Thiadiazole Coordination Polymer as pH Sensor. *J. Lumin.* 210, 38–46. doi:10.1016/j.jlumin.2019.02.014

Fu, W., Liu, L., Yang, G., Deng, L., Zou, B., Ruan, W., et al. (2015). Oleylamine-Assisted Phase-Selective Synthesis of Cu2−x S Nanocrystals and the Mechanism of Phase Control. *Part. Part. Syst. Charact.* 32 (9), 907–914. doi:10.1002/ppsc.201500083

Han, S.-K., Gu, C., Zhao, S., Xu, S., Gong, M., Li, Z., et al. (2016). Precursor Triggering Synthesis of Self-Coupled Sulfide Polymorphs with Enhanced Photoelectrochemical Properties. *J. Am. Chem. Soc.* 138 (39), 12913–12919. doi:10.1021/jacs.6b06609

Hao, R., Peng, Z., and Zhang, B. (2020). Single-Molecule Fluorescence Microscopy for Probing the Electrochemical Interface. *ACS Omega* 5 (1), 89–97. doi:10.1021/acsomega.9b03763

Itzhak, A., Teblum, E., Girshevitz, O., Okashy, S., Turkulets, Y., Burlaka, L., et al. (2018). Digenite (Cu9S5): Layered P-Type Semiconductor Grown by Reactive Annealing of Copper. *Chem. Mater.* 30 (7), 2379–2388. doi:10.1021/acs.chemmater.8b00191

Jing, M., Li, F., Chen, M., Zhang, J., Long, F., Jing, L., et al. (2018). Facile Synthetic Strategy to Uniform Cu9S5 Embedded into Carbon: A Novel Anode for Sodium-Ion Batteries. *J. Alloys Compd.* 762, 473–479. doi:10.1016/j.jallcom.2018.05.224

Khorsand Zak, A., Abd. Majid, W. H., Abrishami, M. E., and Yousefi, R. (2011). X-ray Analysis of ZnO Nanoparticles by Williamson-Hall and Size-Strain Plot Methods. *Solid State. Sci.* 13 (1), 251–256. doi:10.1016/j.solidstatesciences.2010.11.024

Li, S., Cheng, W., Liu, X., Wang, C., Li, W., and Yu, S. (2018). Supercritical Methanol Synthesis, Phase Evolution and Formation Mechanism of Cu1.8S and Cu9S5/CuS Complex Microcrystal. *J. Supercrit. Fluids* 133, 429–436. doi:10.1016/j.supflu.2017.11.007

Li, S., Ge, Z.-H., Zhang, B.-P., Yao, Y., Wang, H.-C., Yang, J., et al. (2016). Mechanochemically Synthesized Sub-5 Nm Sized CuS Quantum Dots with High Visible-Light-Driven Photocatalytic Activity. *Appl. Surf. Sci.* 384, 272–278. doi:10.1016/j.apsusc.2016.05.034

Li, S., Zhang, Z., Yan, L., Jiang, S., Zhu, N., Li, J., et al. (2017). Fast Synthesis of CuS and Cu9S5 Microcrystal Using Subcritical and Supercritical Methanol and Their Application in Photocatalytic Degradation of Dye in Water. *J. Supercrit. Fluids* 123, 11–17. doi:10.1016/j.supflu.2016.12.014

Liu, H., Zhang, H., Wang, J., and Wei, J. (2020). Effect of Temperature on the Size of Biosynthesized Silver Nanoparticle: Deep Insight into Microscopic Kinetics Analysis. *Arabian J. Chem.* 13 (1), 1011–1019. doi:10.1016/j.arabjc.2017.09.004

Liu, M., Liu, Y., Gu, B., Wei, X., Xu, G., Wang, X., et al. (2019). Recent Advances in Copper Sulphide-Based Nanoheterostructures. *Chem. Soc. Rev.* 48 (19), 4950–4965. doi:10.1039/c8cs00832a

Liu, Y., Liu, M., and Swihart, M. T. (2017). Reversible Crystal Phase Interconversion between Covellite CuS and High Chalcocite Cu2S Nanocrystals. *Chem. Mater.* 29 (11), 4783–4791. doi:10.1021/acs.chemmater.7b00579

Malik, M. A., Revaprasadu, N., and O'Brien, P. (2001). Air-Stable Single-Source Precursors for the Synthesis of Chalcogenide Semiconductor Nanoparticles. *Chem. Mater.* 13 (3), 913–920. doi:10.1021/cm0011662

Mazor, H., Golodnitsky, D., Burstein, L., and Peled, E. (2009). High Power Copper Sulfide Cathodes for Thin-Film Microbatteries. *Electrochem. Solid-state Lett.* 12 (12), A232. doi:10.1149/1.3240921

Mbewana-Ntshanka, N. G., Moloto, M. J., and Mubiayi, P. K. (2020). Role of the Amine and Phosphine Groups in Oleylamine and Trioctylphosphine in the Synthesis of Copper Chalcogenide Nanoparticles. *Heliyon* 6 (11), e05130. doi:10.1016/j.heliyon.2020.e05130

Motaung, M. P., Osuntokun, J., and Onwudiwe, D. C. (2019). The Heat-Up Synthesis of Monodispersed Bi2S3 and Cu7S4 Nanoparticles from Novel Precursor Complexes and Their Characterizations. *Mater. Sci. Semiconductor Process.* 99, 92–98. doi:10.1016/j.mssp.2019.04.024

Onwudiwe, D. C., and Ajibade, P. A. (2010). Synthesis and Characterization of Metal Complexes of *N*-Alkyl-*N*-Phenyl Dithiocarbamates. *Polyhedron* 29, 1431–1436. doi:10.1016/j.poly.2010.01.011

Pop, A. E., Popescu, V., Danila, M., and Batin, M. N. (2011). Optical Properties of CuxS Nano-Powders. *Chalcogenide Lett.* 8 (6), 363–370.

Raebiger, H., Lany, S., and Zunger, A. (2007). Origins of the P-type Nature and Cation Deficiency in Cu_2O and Related Materials. *Phys. Rev. B* 76 (4), 045209. doi:10.1103/physrevb.76.045209

Saeed, S., Rashid, N., and Ahmad, K. S. (2013). Aerosol-assisted Chemical Vapor Deposition of Copper Sulfide Nanostructured Thin Film from Newly Synthesized Single-Source Precursor. *Turk J. Chem.* 37, 796–804. doi:10.3906/kim-1210-56

Safrani, T., Jopp, J., and Golan, Y. (2013). A Comparative Study of the Structure and Optical Properties of Copper Sulfide Thin Films Chemically Deposited on Various Substrates. *RSC Adv.* 3 (45), 23066. doi:10.1039/c3ra42528b

Senthilkumar, M., and Babu, S. M. (2016). Crystal Structure Controlled Synthesis and Characterization of Copper Sulfide Nanoparticles. *AIP Conf. Proc.* 1731 (1), 050131.

Shanmugam, M., Sagadevan, A., Charpe, V. P., Pampana, V. K. K., and Hwang, K. C. (2020). Cu 2 O Nanocrystals-Catalyzed Photoredox Sonogashira Coupling of Terminal Alkynes and Arylhalides Enhanced by CO 2. *ChemSusChem* 13 (2), 287–292. doi:10.1002/cssc.201901813

Shiga, Y., Umezawa, N., Srinivasan, N., Koyasu, S., Sakai, E., and Miyauchi, M. (2016). A Metal Sulfide Photocatalyst Composed of Ubiquitous Elements for Solar Hydrogen Production. *Chem. Commun.* 52 (47), 7470–7473. doi:10.1039/c6cc03199d

Suárez, J. A., Plata, J. J., Márquez, A. M., and Sanz, J. F. (2017). Effects of the Capping Ligands, Linkers and Oxide Surface on the Electron Injection Mechanism of Copper Sulfide Quantum Dot-Sensitized Solar Cells. *Phys. Chem. Chem. Phys.* 19 (22), 14580–14587. doi:10.1039/c7cp01076a

Tauc, J., Grigorovici, R., and Vancu, A. (1966). Optical Properties and Electronic Structure of Amorphous Germanium. *Phys. Stat. Sol. (B)* 15 (2), 627–637. doi:10.1002/pssb.19660150224

Tyagi, A., Kole, G. K., Shah, A. Y., Wadawale, A., Srivastava, A. P., Kumar, M., et al. (2019). Accessing Copper-Tin-Sulfide Nanostructures from Diorganotin(IV) and Copper(I) 2-pyrazinyl Thiolates. *J. Organomet. Chem.* 887, 24–31. doi:10.1016/j.jorganchem.2019.02.026

Wang, Y., Liu, F., Ji, Y., Yang, M., Liu, W., Wang, W., et al. (2015). Controllable Synthesis of Various Kinds of Copper Sulfides (CuS, Cu7S4, Cu9S5) for High-Performance Supercapacitors. *Dalton Trans.* 44 (22), 10431–10437. doi:10.1039/c5dt00402k

Yoo, S. H., and Kim, C. K. (2009). Nanocomposite Encapsulation of CuS:Eu Light-Emitting Diode Phosphors for the Enhancement of the Stability Against Moisture. *J. Electrochem. Soc.* 156 (7), J170. doi:10.1149/1.3121730

Yue, H. Y., Zhang, H. J., Huang, S., Lu, X. X., Gao, X., Song, S. S., et al. (2020). Highly Sensitive and Selective Dopamine Biosensor Using Au Nanoparticles-ZnO Nanocone Arrays/graphene Foam Electrode. *Mater. Sci. Eng. C.* 108, 110490. doi:10.1016/j.msec.2019.110490

Zhang, K., Khan, M. W., Zuo, X., Yang, Q., Tang, H., Wu, M., et al. (2019). Controllable Synthesis and Photoelectric Properties of Interconnected and Self-Assembled Nanocomposite of Porous Hollow Cu7S4/CuS and Nitrogen-Doped Graphene Oxide. *Electrochimica. Acta.* 307, 64–75. doi:10.1016/j.electacta.2019.03.173

Zhang, Y., Qiao, Z.-P., and Chen, X.-M. (2002). Microwave-Assisted Elemental-Direct-Reaction Route to Nanocrystalline Copper Sulfides Cu9S8 and Cu7S4. *J. Solid State. Chem.* 167 (1), 249–253. doi:10.1006/jssc.2002.9656

Zhao, J., Wang, S., Zhang, S., Zhao, P., Wang, J., Yan, M., et al. (2020). Peptide Cleavage-Mediated Photoelectrochemical Signal On-Off via CuS Electronic Extinguisher for PSA Detection. *Biosens. Bioelectron.* 150, 111958. doi:10.1016/j.bios.2019.111958

Zhao, Y., Pan, H., Lou, Y., Qiu, X., Zhu, J., and Burda, C. (2009). Plasmonic Cu2−xS Nanocrystals: Optical and Structural Properties of Copper-Deficient Copper(I) Sulfides. *J. Am. Chem. Soc.* 131 (12), 4253–4261. doi:10.1021/ja805655b

Zhu, H., and Wang, L. (2019). Smart Window Based on Cu7S4/hydrogel Composites with Fast Photothermal Response. *Solar Energ. Mater. Solar Cell* 202, 110109. doi:10.1016/j.solmat.2019.110109

Conflict of Interest: The authors declare that the research was conducted in the absence of any commercial or financial relationships that could be construed as a potential conflict of interest.